Proc. Natl. Acad. Sci. USA
Vol. 93, pp. 4907–4912, May 1996
Biochemistry

Using ubiquitin to follow the metabolic fate of a protein

(proteolysis/pulse-chase/half-life/N-end rule/cell culture)

FRÉDÉRIC LÉVY, NILS JOHNSSON*, TILLMANN RÜMENAPF†, AND ALEXANDER VARSHAVSKY‡

Division of Biology, California Institute of Technology, Pasadena, CA 91125

Contributed by Alexander Varshavsky, December 15, 1995

ABSTRACT We describe a method that can be used to produce equimolar amounts of two or more specific proteins in a cell. In this approach, termed the ubiquitin/protein/reference (UPR) technique, a reference protein and a protein of interest are synthesized as a polyprotein separated by a ubiquitin moiety. This tripartite fusion is cleaved, cotranslationally or nearly so, by ubiquitin-specific processing proteases after the last residue of ubiquitin, producing equimolar amounts of the protein of interest and the reference protein bearing a C-terminal ubiquitin moiety. In applications such as pulse-chase analysis, the UPR technique can compensate for the scatter of immunoprecipitation yields, sample volumes, and other sources of sample-to-sample variation. In particular, this method allows a direct comparison of proteins' metabolic stabilities from the pulse data alone. We used UPR to examine the N-end rule (a relation between the *in vivo* half-life of a protein and the identity of its N-terminal residue) in L cells, a mouse cell line. The increased accuracy afforded by the UPR technique underscores insufficiency of the current "half-life" terminology, because *in vivo* degradation of many proteins deviates from first-order kinetics. We consider this problem and discuss other applications of UPR.

Ubiquitin (Ub) is a 76-residue protein that exists in cells either free or covalently linked to many different proteins. Ub-protein conjugation is involved (directly or by way of regulation) in a multitude of processes, including cell growth and division, signal transduction, DNA repair, and the transport of substances across membranes. In many of these processes, Ub acts through routes that involve the degradation of Ub-protein conjugates (1, 2). The linking of Ub to other proteins involves the formation of an isopeptide bond between the C-terminal glycine of Ub and the ε-amino group of a Lys residue in an acceptor protein. Unlike the resulting branched Ub-protein conjugates, which are formed posttranslationally, linear Ub adducts are formed as the translational products of natural or engineered Ub fusions (2, 3).

A newly formed Ub fusion such as Ub-X-β-galactosidase (Ub-X-βgal) is rapidly (cotranslationally or nearly so) cleaved at the Ub-protein junction by Ub-specific processing proteases (UBPs) (4, 5) regardless of the identity of a residue X at the C-terminal side of the cleavage site, proline being the single exception (2, 6). The relation between the metabolic stability of a resulting protein and the identity of its N-terminal residue is called the N-end rule (2). The N-end rule pathway has been shown to operate in the eubacterium *Escherichia coli* (7), in the yeast *Saccharomyces cerevisiae* (8), and in ATP-supplemented extract from rabbit reticulocytes (9). The N-end rules of these organisms are similar but not identical (2). The degradation signal recognized by the N-end rule pathway is called the N-degron. This signal comprises two determinants: a destabilizing N-terminal residue and a specific internal lysine (or lysines) of a protein substrate (2, 8). The Lys residue is the site of formation of a substrate-linked multi-Ub chain, whose presence is required for the degradation of N-end rule substrates by the proteasome—an ATP-dependent, multisubunit protease (10).

The N-end rule is organized hierarchically. In eukaryotes such as the yeast *S. cerevisiae*, Asn and Gln are tertiary destabilizing N-terminal residues in that they function through their conversion, by a specific amidase, into the secondary destabilizing residues Asp and Glu, whose activity requires their conjugation, by Arg-tRNA-protein transferase (R-transferase), to Arg, one of primary destabilizing N-terminal residues (2, 11). The latter are bound directly by a protein called N-recognin or E3. In *S. cerevisiae*, N-recognin is a 225-kDa protein (encoded by *UBR1*) that selects potential N-end rule substrates by binding to their primary destabilizing N-terminal residues, Phe, Leu, Trp, Tyr, Ile, Arg, Lys, or His (2). The only known metazoan N-end rule, determined not *in vivo* but in ATP-supplemented extract from rabbit reticulocytes, differs from the yeast N-end rule (9). In particular, Cys, which is a stabilizing residue in *S. cerevisiae* (8), is a secondary destabilizing residue in reticulocytes (9).

The understanding of N-end rule's functions remains sketchy. The N-end rule pathway has been shown to be required for the import of peptides in *S. cerevisiae* (12). It is also required for the degradation of yeast Gα, the *GPA1*-encoded α subunit of the heterotrimeric G protein (13). Sindbis virus RNA polymerase is another physiological substrate of the N-end rule pathway (14).

Determination of an N-end rule entails multiple pulse-chase assays. A pulse-chase analysis involves the labeling of nascent proteins for a short time with a radioactive precursor ("pulse"), the termination of labeling, and the analysis of a labeled protein of interest at various times afterwards ("chase"), using immunoprecipitation and SDS/PAGE, or analogous techniques. Its advantage of being direct notwithstanding, a conventional pulse-chase assay is fraught with sources of error. For example, the immunoprecipitation yields may vary from sample to sample; the volumes of samples loaded on a gel may vary as well. As a result, pulse-chase data tend to be semiquantitative at best, lacking the means to control these errors. Prompted in part by the necessity to improve the procedure for determining the N-end rule, we developed a robust and convenient "internal reference" strategy that can compensate for at least some of the data scatter in a pulse-chase assay.

Described below is a modification of the original Ub fusion design (2, 6) that can be used to produce equimolar amounts of two (or more) specific proteins in a cell. We apply this method, termed the ubiquitin/protein/reference (UPR) technique, to the pulse-chase assay and illustrate the utility of UPR by determining the N-end rule in L cells, a fibroblast-like mouse cell line.

Abbreviations: Ub, ubiquitin (or ubiquityl moiety); UPR, ubiquitin/protein/reference; UBP, ubiquitin-specific processing protease; βgal, *E. coli* β-galactosidase; DHFR, dihydrofolate reductase; ID, initial decay; SD, subsequent decay.

*Present address: Max-Delbrück-Laboratorium, Carl-von-Linné-Weg 10, D-50829 Köln, Germany.
†Present address: Justus-Liebig-Universität, Institüt für Virologie, Fachbereich Veterinärmedizin, Frankfurter Str. 107, 35392 Giessen, Germany.
‡To whom reprint requests should be addressed at: Division of Biology, 147-75, California Institute of Technology, Pasadena, CA 91125. e-mail: varshavskya@starbase1.caltech.edu.

The publication costs of this article were defrayed in part by page charge payment. This article must therefore be hereby marked "*advertisement*" in accordance with 18 U.S.C. §1734 solely to indicate this fact.

MATERIALS AND METHODS

Construction of Plasmids. Details are available upon request. A set of ORFs encoding Ub-X-nsP4 was described (15) (see also *Results*). The nsP4-coding sequence (14) was shortened to encode the first 165 residues of nsP4, and the resulting fragment was ligated, in-frame, to *E. coli lacZ* encoding βgal that lacked the first six residues. The *Xba*I–*Stu*I fragment encoding Ub-X-$nsP4_{165}$-βgal (the $nsP4_{165}$ portion of this and related constructs is denoted below as nsP4) was blunted with the Klenow fragment of DNA polymerase I and inserted into the blunted *Hin*dIII site of the pRC/CMV vector (Invitrogen), yielding the plasmids pRC/UbXnsP4βgal that differed at codons encoding the residue X of Ub-X-nsP4-βgal. An *Xba*I–*Sac*II fragment encoding dihydrofolate reductase (DHFR)-ha-Ub^{R48} was constructed by a multistep PCR. This fragment was inserted into *Xba*I–*Sac*II-cut pRc/UbXnsP4βgal plasmids, yielding the plasmids pRc/dhaUbXβgal that expressed DHFR-ha-Ub^{R48}-X-nsP4-βgal (dha-Ub-X-βgal) test proteins from the P_{CMV} promoter (16).

Cell Culture, Transfection, and Pulse-Chase Analysis. L cells (ATCC CCL 1.3), a line of transformed, fibroblast-like mouse cells, were grown as monolayers in the DMEM/F12 medium (GIBCO) supplemented with 10% fetal bovine serum, antibiotics, 2 mM L-glutamine, and 20 mM NaHepes (pH 7.3). The plasmids pRc/dhaUbXβgal were introduced into L cells using Lipofectamine (GIBCO) and the manufacturer-supplied protocol. After 16 hr at 37°C, a DNA-containing solution in each 3.5-cm plate was replaced by 1 ml of serum-free medium lacking methionine and cysteine and, after 30 min, by 0.5 ml of serum-free medium containing 0.1 mCi (1 Ci = 37 GBq) of ^{35}S-Express (New England Nuclear), followed by incubation for 10 min at 37°C. Immediately thereafter, the plates were washed with 1 ml of complete medium, the "time-zero" plate was processed as described below, and 1 ml of the chase medium (complete medium plus cycloheximide at 0.1 mg/ml) was added to each of the other plates. At each time point, the chase medium was aspirated, 1 ml of ice-cold buffer A (1% Triton X-100/0.15 M NaCl/5 mM EDTA/0.2 mg/ml phenylmethylsulfonyl fluoride/20 mM Tris·HCl, pH 7.5) was added, and the plate was placed on ice. The lysates were collected and centrifuged at 12,000 × *g* for 1 min. The volumes of supernatants were adjusted to contain equal amounts of 10% trichloroacetic acid-insoluble ^{35}S, followed by immunoprecipitation with a mixture of saturating amounts of monoclonal antibodies against the ha epitope (Babco, Emeryville, CA) and βgal (Promega). The samples were incubated, with rotary shaking, at 4°C for 30 min, followed by the addition of Protein A-Sepharose (Repligen) and another 30-min incubation at 4°C. The immunoprecipitates were washed three times in buffer A plus 0.1% SDS, resuspended in 20 μl of SDS-sample buffer (16), and heated at 100°C for 3 min. The samples were subjected to SDS/12% PAGE (16), followed by autoradiography with x-ray films and, independently, quantitation using a PhosphorImager (Molecular Dynamics).

RESULTS

The UPR Technique. The strategy of UPR is illustrated in Fig. 1*A*. Previous work (6, 8) has shown that Ub fusions containing a sterically accessible Ub moiety and expressed at moderate levels are cleaved rapidly enough for the amounts of uncleaved fusion to be negligible even at pulse times comparable with the time required for the fusion's translation (6, 8). Another study (17) explored kinetic aspects of protein transport across membranes by using fusions that bore a signal sequence and a Ub moiety embedded between two other protein domains. Fusions of this design that could not be cotranslationally translocated into the endoplasmic reticulum were cleaved at the Ub-protein junction in the cytosol, indicating that the presence of an N-terminal extension in the fusion's Ub moiety did not interfere with the fusion's cleavage (17).

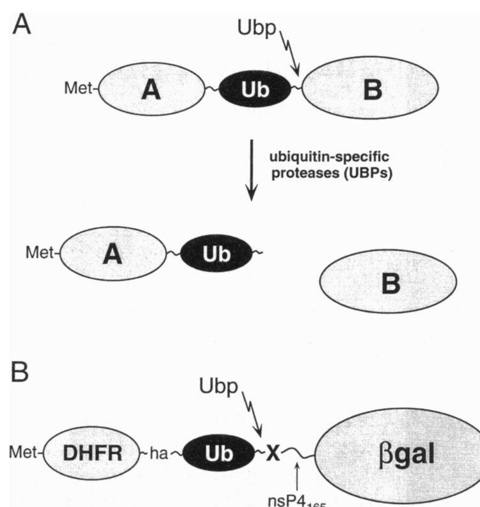

FIG. 1. The UPR technique. (*A*) A tripartite fusion containing A, a reference protein moiety whose C-terminus is linked, via a spacer peptide, to a Ub moiety. The C-terminus of Ub is linked to B, a protein of interest. *In vivo*, this tripartite fusion is cleaved, cotranslationally or nearly so, by UBPs at the Ub-B junction, yielding equimolar amounts of the unmodified protein B and the reference protein A bearing a C-terminal Ub moiety. If protein A-Ub is long-lived, determining the ratio of A-Ub to B as a function of time or at steady state yields, respectively, the *in vivo* decay curve or the relative metabolic stability of protein B. (*B*) In UPR assays of the present work, the reference protein was mouse DHFR, linked, via a 20-residue spacer containing the ha epitope (16), to the Ub moiety bearing arginine instead of wild-type lysine at position 48. The Ub^{R48} moiety was fused to the test protein, a modified *E. coli* βgal bearing a varied residue (X) at the Ub-βgal junction, and a 165-residue insert, derived from the Sindbis virus nsP4 protein, between X and βgal (see *Results*). The resulting fusion is denoted as DHFR-ha-Ub^{R48}-X-nsP4-βgal or, briefly, as dha-Ub-X-βgal.

Thus, by expressing a fusion whose Ub moiety is located between polypeptides A and B, it should be possible to produce, cotranslationally or nearly so, equimolar amounts of two separate polypeptides, A-Ub and B (Fig. 1*A*). One application of this approach, termed the UPR technique, is to employ A-Ub as a reference protein in a pulse-chase assay, with B as a test protein.

UPR and the N-End Rule. The development of the UPR technique was prompted in part by insufficient reproducibility of conventional pulse-chase assays in studies of the N-end rule (see the Introduction), and also by the necessity of estimating the degradation of N-end rule substrates and other short-lived proteins *during* the pulse (see below). The utility of UPR was tested by using it to determine the N-end rule in L cells, a fibroblast-like mouse cell line.

A UPR-based protein fusion used to determine the N-end rule in mammalian cells comprised, starting from the N-terminus: the 21-kDa mouse DHFR moiety; a 20-residue linker containing the ha epitope (recognized by a monoclonal antibody); a modified Ub moiety (Ub^{R48}) in which lysine at position 48 had been replaced by arginine; a variable residue X after the last residue of Ub^{R48}; and the 116-kDa *E. coli* βgal that lacked the first six residues of wild-type βgal and bore a 165-residue N-terminal extension derived from nsP4, the Sindbis virus RNA polymerase. The entire fusion, DHFR-ha-Ub^{R48}-X-nsP4-βgal, is denoted below as dha-Ub-X-βgal (Fig. 1*B*). The *in vivo* cleavage of this fusion produced dha-Ub (DHFR-ha-Ub^{R48}), which served as a reference protein, and X-βgal (X-nsP4-βgal), which served as a test N-end rule substrate, X being the variable N-terminal residue (Fig. 1*B*).

The use of Ub^{R48} instead of wild-type Ub in dha-Ub-X-βgal was expected to preclude the possibility of C-terminal Ub moiety in

dha-Ub acting as a ubiquitylation§/degradation signal [Lys-48 of Ub is one major site of the Ub-Ub isopeptide bonds within a multi-Ub chain, whereas an Arg residue cannot be ubiquitylated (1)]. The 165-residue nsP4 insert corresponds to the N-terminal region of the 70-kDa nsP4 (Sindbis virus RNA polymerase), one physiological substrate of the N-end rule pathway (14). The function of the nsP4-derived insert in X-nsP4-βgal (X-βgal) was to provide the second (internal-lysine) determinant of the N-degron. The previously used lysine-bearing insert in X-βgal was a 45-residue sequence derived from *E. coli* Lac repressor (8). This insert functions well in yeast (6, 8) but was ineffective in mammalian cells (data not shown). We do not understand the cause of this difference in the relative strength of a given N-degron between yeast and mammalian cells.

Data Scatter and Its Correction by UPR. Mouse L cells were transiently transfected with plasmids expressing dha-Ub-Met-βgal or dha-Ub-Arg-βgal (Fig. 1*B*). The cells were labeled for 10 min at 37°C with [^{35}S]methionine/cysteine, followed by the addition of cycloheximide (to inhibit translation) and a chase of 60 and 120 min. Each sample was processed for immunoprecipitation and SDS/PAGE using a mixture of anti-ha and anti-βgal antibodies (Fig. 2). In one such experiment, the amount of ^{35}S in Met-βgal at 60 min of chase was 60% of the amount at time 0 (at the end of the 10-min pulse) (Fig. 2*A*, lanes a–c, and *B*, open circles), consistent with the possibility that a large fraction of labeled Met-βgal was degraded during the 60-min chase. However, when the amount of ^{35}S in Met-βgal was normalized against the amount of ^{35}S in the reference protein dha-Ub of the same sample, and the resulting ratios were plotted as percentages of the ratio at time 0 (Fig. 2*B*, closed circles), it became clear that the relative amount of pulse-labeled Met-βgal was in fact nearly constant during the chase, in agreement with earlier evidence that methionine is a stabilizing residue in the N-end rule (2, 8, 9).

The amount of ^{35}S in Arg-βgal, whose N-terminal arginine is a destabilizing residue in all of the known N-end rules (9), at time 0 was only 11% of the amount of ^{35}S in Met-βgal (Fig. 2*A*, lane d vs. lane a, and *B*, open triangles vs. open circles). The amount of ^{35}S in Arg-βgal continued to decrease during the chase (Fig. 2 *A*, lanes d–f, and *B*, open triangles). These "raw" values for the amounts of ^{35}S in Arg-βgal were normalized against the amount of ^{35}S in the reference protein dha-Ub of the same samples, and the corresponding ratios were plotted as percentages of the analogous ratio for Met-βgal at time 0. Both the shape and the initial (time-zero) values of the resulting decay curve for Arg-βgal differed significantly from those of the uncorrected curve (Fig. 2*B*). The much lower amount of ^{35}S in Arg-βgal than in Met-βgal at time 0 (Fig. 2*B*) resulted from extensive degradation of Arg-βgal during the 10-min pulse (see below).

The N-End Rule in Mouse L-Cells. The pulse-chase assays of Fig. 2 were expanded to include 19 plasmids expressing UPR-based dha-Ub-X-βgal (DHFR-ha-Ub^{R48}-X-nsP4-βgal) fusions, X being a variable residue (Fig. 1*B*). Pro was the only N-terminal residue absent from the set of resulting X-βgal test proteins, because a Ub-Pro-bearing fusion is deubiquitylated slowly in either yeast or mammalian cells (6, 9). Depending on the identity of X in X-βgal proteins, these proteins were either long-lived or metabolically unstable (Fig. 3). These measurements, carried out with 19 X-βgals, yielded the N-end rule in mouse L cells (Figs. 3 and 4, and Table 1).

As noted earlier (6, 18), the *in vivo* decay curves of pulse-labeled, short-lived X-βgals deviated from first-order kinetics, in that the metabolic stability of older X-βgal molecules was higher than the metabolic stability of their younger counterparts (Fig. 3). For example, the degradation of a short-lived X-βgal was in all cases more rapid during the first 60 min of chase than during the next 60 min (Fig. 3). (Control experiments have shown that the kinetics of X-βgal degradation was not influenced significantly by the presence of cycloheximide during the chase.) Analysis of X-βgal decay using the chase times of 15, 30, and 60 min (Fig. 3*D*) instead of 60 and 120 min (Fig. 3 *A–C*) indicated that the degradation of pulse-labeled X-βgals was strongly diminished by 15 min of chase (Fig. 3*D*).

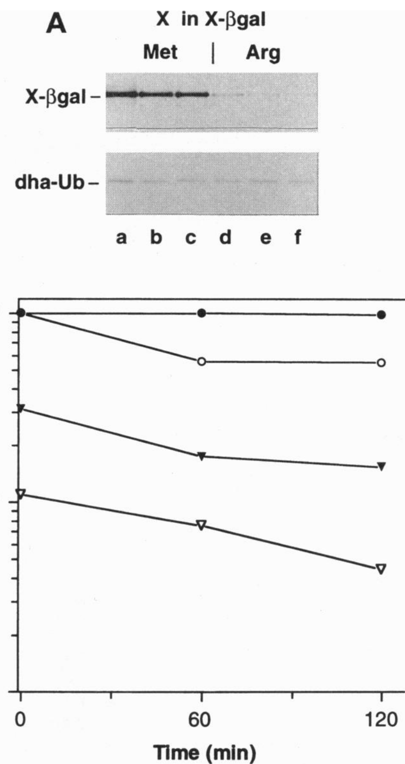

FIG. 2. The use of UPR to compensate for data scatter in a pulse-chase assay. (*A*) Mouse L cells were transfected with plasmids expressing dha-Ub-X-βgal, the residue X being methionine or arginine. Cells were labeled for 10 min with [^{35}S]methionine/cysteine and chased for 0 (lanes a and d), 60 (lanes b and e), and 120 min (lanes c and f), followed by preparation of extracts, immunoprecipitation with anti-ha and anti-βgal antibodies, SDS/PAGE, and autoradiography (see *Materials and Methods*). The bands of X-βgal (test proteins) and dha-Ub (reference protein) are indicated on the left. (*B*) The pattern in *A* was quantified using a PhosphorImager. ○, ▽, the amount of ^{35}S in, respectively, Met-βgal and Arg-βgal during the chase, plotted as a percentage of the amount of ^{35}S in Met-βgal at time 0 (at the end of pulse). ●, at each time point, the ratio of ^{35}S in Met-βgal to ^{35}S in dha-Ub was determined, and was plotted as a percentage of this ratio at time 0. ▼, the same as ● but for Arg-βgal, with the resulting ratios plotted as percentages of the Met-βgal/dha-Ub ratio at time 0.

Another distinct feature of the decay curves was that the relative amount of ^{35}S in a short-lived X-βgal at time 0 (the end of the 10-min pulse) was always lower than the time-zero amount of ^{35}S in a long-lived X-βgal such as Met-βgal (Fig. 3). Low yields of short-lived X-βgals at time 0 were caused by their degradation during the pulse; this feature of X-βgal decay curves was referred to as a "zero-point" effect (18). The use of UPR-based constructs (Fig. 1) instead of the earlier, reference-lacking test proteins increased the accuracy (reproducibility) of pulse-chase assays to an extent that the comparison of (normalized) time-zero values for different X-βgals could be used to rank their metabolic stabilities, yielding the N-end rule diagram of Fig. 4.

A Constant-Pulse Assay. In this assay, proteins were labeled continuously, without a chase (Fig. 5). The ratio of ^{35}S in Met-βgal to ^{35}S in the reference protein dha-Ub increased greatly

§To bring ubiquitin-related terms in line with the standard chemical terminology, ubiquitin whose C-terminal (Gly-76) carboxyl group is covalently linked to another compound will be called the ubiquityl moiety, with the derivative terms being ubiquitylation and ubiquitylated instead of the earlier terms "ubiquitination" and "ubiquitinated" (1–3). The abbreviation Ub will refer to both free ubiquitin and the ubiquityl moiety.

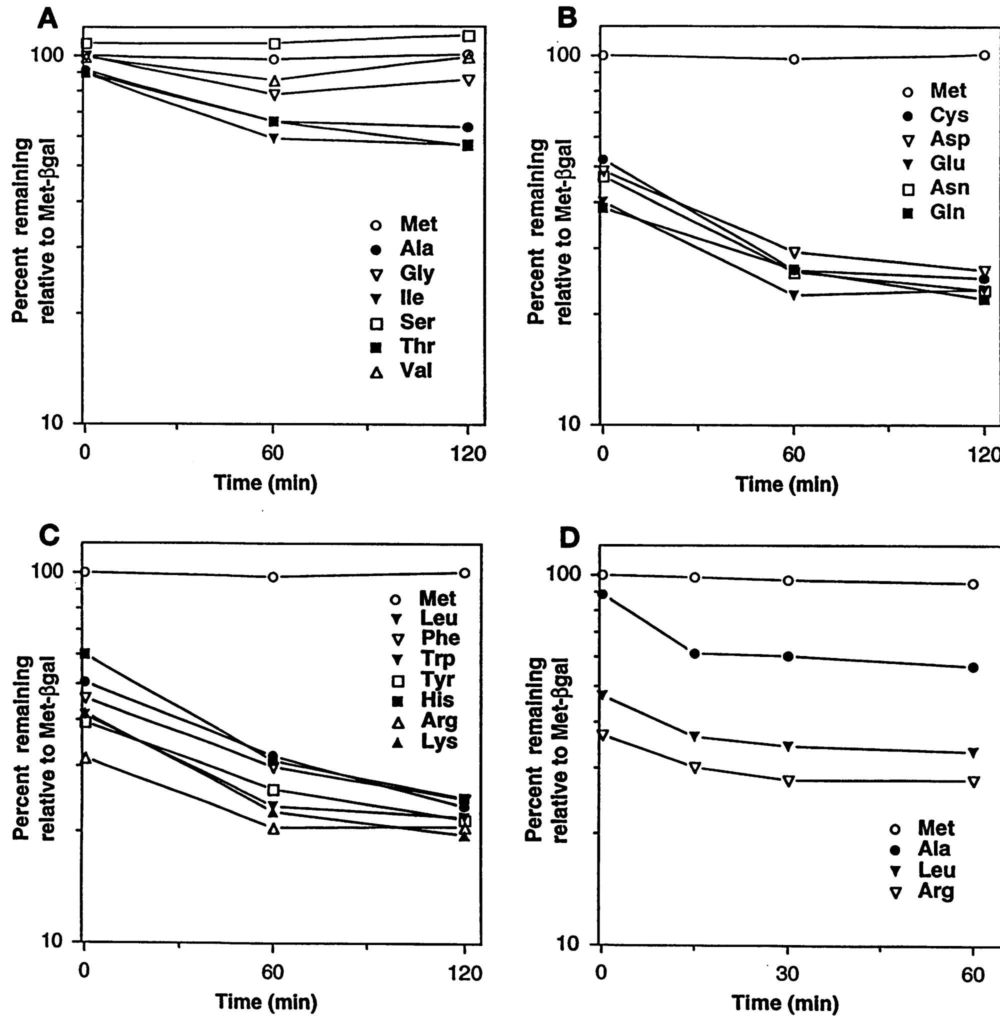

FIG. 3. *In vivo* degradation of X-βgal test proteins. UPR-based pulse-chase assays were carried out as described in *Materials and Methods* to follow the degradation of X-βgal test proteins (produced from dha-Ub-X-βgals) in mouse L cells. The relative amounts of ^{35}S in X-βgals, defined, at each time point, as the ratio of ^{35}S in an X-βgal to dha-Ub (the reference protein), were plotted as percentages of the same ratio at time 0 for Met-βgal. Each of the decay curves shown is the average of two independent UPR assays, whose results differed by less than 10%. (*A*) X = Met, Ala, Gly, Ile, Ser, Thr, and Val residues. (*B*) X = Met, Cys, Asp, Glu, Asn, and Gln residues. (*C*) X = Met, Leu, Phe, Trp, Tyr, His, Arg, and Lys residues. (*D*) X = Met, Ala, Leu, and Arg residues, the chase times being 15, 30, and 60 min (instead of 60 and 120 min).

between 5 and 10 min of pulse, reaching a near-plateau by 20 min (Fig. 5, open circles). The analogous ratio for Arg-βgal showed similar kinetics of increase but with a lower plateau (≈35% of the value for Met-βgal) (Fig. 5, closed circles). The total incorporation of ^{35}S into proteins remained linear from 5 to at least 80 min of pulse (Fig. 5, open squares), precluding the possibility that the ratio curves in Fig. 5 could be caused by a decrease in the total incorporation of ^{35}S during the pulse.

A parsimonious interpretation of these results is that the 28-kDa dha-Ub reference moiety (seven Met residues), which emerges from the ribosome before the 140-kDa Met-βgal moiety (26 Met residues) of dha-Ub-Met-βgal, is overrepresented as a full-length polypeptide during the earliest times of pulse, because it takes ≈0.3 min to synthesize dha-Ub but ≈1.5 min to synthesize Met-βgal (assuming the rate of translation to be ≈15 residues per second under the conditions used). The contribution of this difference in translation rates between dha-Ub and Met-βgal to the ratio of ^{35}S incorporation into these proteins should progressively decrease during the pulse, resulting in a nearly constant ratio at the durations of pulse that are much longer than the translation times, as observed (Fig. 5, open circles). The shape of the analogous curve for Arg-βgal is similar to, but the plateau value is only 35% of the value for, Met-βgal (Fig. 5, closed vs. open circles), reflecting the degradation of Arg-βgal.

DISCUSSION

In the UPR technique, a Ub moiety is placed between polypeptides A and B within a linear fusion. *In vivo*, this fusion is cleaved, cotranslationally or nearly so, at the Ub-B junction, yielding equimolar amounts of two separate polypeptides, A-Ub and B (Fig. 1*A*). More generally, by positioning n Ub moieties within a fusion, one can produce equimolar amounts of $n + 1$ separate polypeptides in a cell. The UPR technique has advantages over other ways of attaining this goal. For

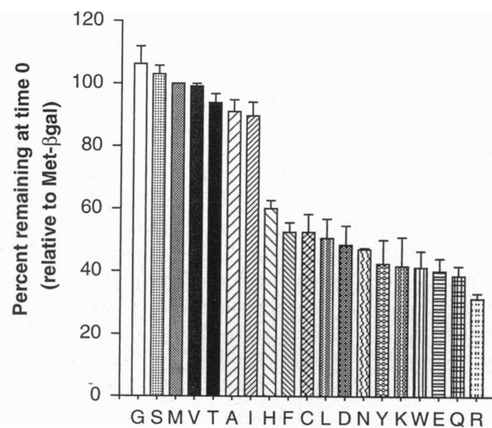

FIG. 4. The N-end rule in mouse L cells. The relative amounts of X-βgal test proteins immediately after the 10-min pulse (time 0) were determined using dha-Ub-X-βgal fusions (Fig. 1*B*) and the UPR-based assay as described in *Materials and Methods* (see also the legend to Fig. 3). The resulting values (averaged from three independent experiments) were plotted (as percentages of the relative amount of Met-βgal) for all N-terminal residues in X-βgal except the Pro residue. Standard deviations are indicated above the bars. Single-letter abbreviations of amino acids: A, Ala; C, Cys; D, Asp; E, Glu; F, Phe; G, Gly; H, His; I, Ile; K, Lys; L, Leu; M, Met; N, Asn; Q, Gln; R, Arg; S, Ser; T, Thr; V, Val; W, Trp; Y, Tyr.

Table 1. Parameters of X-βgal degradation in mouse L-cells

N-terminal residues	ID^{10}, %	SD^{0-60}, %	$t_{0.5}^{0-60}$, min	$t_{0.5}^{0-15}$, min
Met	0	2.3 ± 3.3	>120	>120
Ser	0*	0	>120	
Gly	0*	21.9 ± 1.9	>120	
Val	0.9 ± 0.8	13.7 ± 3.0	>120	
Ala	8.9 ± 3.8	27.7 ± 1.4	108	24
Ile	10.3 ± 4.4	33.7 ± 0.2	69	
Thr	10.5 ± 5.2	26.5 ± 3.8	92	
His	39.9 ± 2.6	48.4 ± 0.6	62	
Cys	47.5 ± 5.7	49.6 ± 0.6	60	
Leu	49.4 ± 6.1	37.2 ± 3.1	81	32
Asp	51.3 ± 6.4	39.6 ± 3.5	76	
Asn	52.9 ± 0.5	44.9 ± 1.7	67	
Phe	54.2 ± 8.6	34.7 ± 4.5	86	
Lys	58.3 ± 9.3	45.8 ± 4.5	65	
Trp	58.8 ± 5.2	43.0 ± 2.3	70	
Glu	59.9 ± 4.1	43.9 ± 2.8	68	
Tyr	60.6 ± 4.5	34.1 ± 0.2	88	
Gln	61.4 ± 3.2	31.6 ± 2.9	95	
Arg	68.5 ± 1.6	34.8 ± 3.0	86	26

$[X\text{-}\beta gal]_0$, the "normalized" amount of an X-βgal at time 0 (at the end of the 10-min pulse), was determined by dividing the mean density of PhosphorImager-detected pixels in the electrophoretic band of X-βgal by the mean density of pixels in the band of the reference protein dha-Ub in the same lane. Initial decay of X-βgal at the end of the 10-min pulse (ID^{10}) was calculated as follows: $ID^{10} = 100\% - \{[X\text{-}\beta gal]_0/[Met\text{-}\beta gal]_0\} \times 100\%$. Subsequent decay of X-βgal at 60 min of chase (SD^{0-60}) was calculated as follows: $SD^{0-60} = 100\% - \{[X\text{-}\beta gal]_{60}/[X\text{-}\beta gal]_0\} \times 100\%$, where $[X\text{-}\beta gal]_{60}$ was the normalized amount of X-βgal at 60 min of chase. $t_{0.5}^{0-60}$, the "partial" half-life of an X-βgal between 0 and 60 min of chase, was calculated from the values of $[X\text{-}\beta gal]_{60}$ and $[X\text{-}\beta gal]_0$ by assuming a first-order kinetics of degradation between these time points. Analogous calculations were used to yield $t_{0.5}^{0-15}$, the partial half-life of an X-βgal between 0 and 15 min of chase. The zero values of ID^{10} for Ser-βgal and Gly-βgal are marked by asterisks to denote the fact that the relative amount of ^{35}S in these X-βgals at time 0 was marginally higher than that in Met-βgal (Figs. 3*A* and 4).

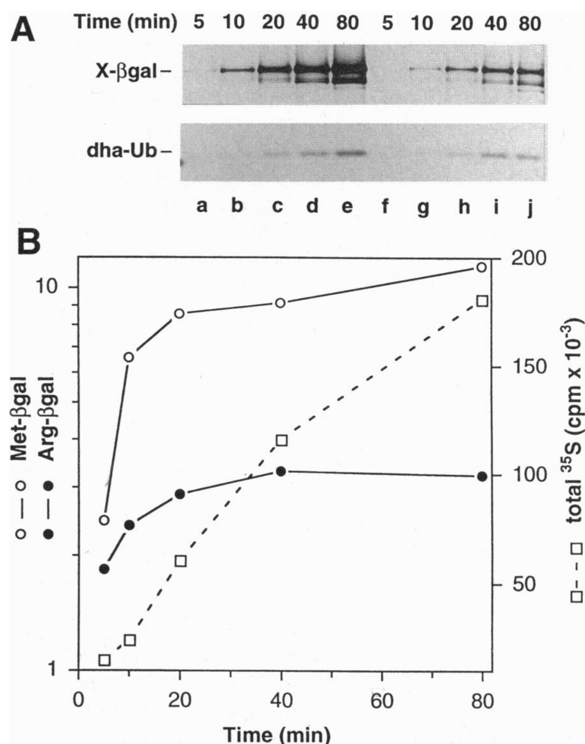

FIG. 5. The UPR-based continuous pulse assay. (*A*) L cells were transfected with plasmids expressing Met-βgal (dha-Ub-Met-βgal) (lanes a–e) or Arg-βgal (dha-Ub-Arg-βgal) (lanes f–j). The cells were labeled with [^{35}S]methionine/cysteine for 5 min (lanes a and f), 10 min (lanes b and g), 20 min (lanes c and h), 40 min (lanes d and i), and 80 min (lanes e and j), followed by the preparation of extracts, immunoprecipitation with anti-ha and anti-βgal antibodies, SDS/PAGE, and autoradiography (see *Materials and Methods*). (*B*) The pattern in *A* was processed for quantitation using a PhosphorImager. ○, the ratio of Met-βgal to dha-Ub during the continuous pulse. ●, the same as ○ but for Arg-βgal. □, total ^{35}S in the 10% trichloroacetic acid-insoluble fraction during the continuous pulse.

example, although cytosolic processing proteases such as viral proteases can also generate equimolar amounts of cleavage products from a polyprotein precursor, these proteases lack the advantages of UBPs (i.e., their universal presence among eukaryotes, their cotranslational cleavage kinetics, and their lack of toxicity upon expression in organisms such as eubacteria that lack the Ub system). A virus-derived, peptide-size insert was reported to function as a cotranslationally cleaving, cis-acting protease within a polyprotein (19); this feature of the insert may yield an analog of the UPR technique.

UPR, Pulse-Chase, and the N-End Rule. To test the utility of UPR, we used it to determine the N-end rule in fibroblast-like mouse L cells. Save for one residue, this *in vivo*-defined mammalian N-end rule (Figs. 3 and 4; Table 1) is identical to the N-end rule of rabbit reticulocytes that had been determined in ATP-supplemented reticulocyte extract (9). The exceptional residue is Ser, which is stabilizing in L cells (Fig. 4) but is destabilizing in reticulocyte extract (9). N-terminal serine is often acetylated *in vivo* (20); it is unknown, thus far, whether N-terminal serine of Ser-βgal is acetylated in L cells. Because acetylation of a destabilizing N-terminal residue is expected to abolish its recognition by the N-end rule pathway (2), it remains to be seen whether the difference in destabilizing activity between N-terminal serine in reticulocytes (9) and in fibroblast-like L cells (Figs. 3*A* and 4) defines a difference between the N-end rules of these cells or whether it is an artifact of inefficient acetylation of N-terminal serine in reticulocyte extract. Among destabilizing residues in the L cell N-end rule, Ile, Ala, and Thr are the least destabilizing ones (Fig. 3, compare *A* with *B*).

In contrast to the *S. cerevisiae* and *E. coli* N-end rules, where cysteine is a stabilizing residue (2), cysteine is clearly destabilizing in both mouse L cells and rabbit reticulocytes (Figs. 3 and 4; ref. 12). RNAase digestion and [^{3}H]arginine incorporation tests in reticulocyte extract showed cysteine to be a secondary destabilizing residue in reticulocytes (9) (see the Introduction for the terminology). Whether cysteine is also a secondary destabilizing residue in L cells remains to be determined. Unlike the other moderately or strongly destabilizing residues (Fig. 4), cysteine can be exposed at the N-terminus of a protein through a cleavage by the known Met-aminopeptidases (20). Indeed, Met-Cys-βgal was as metabolically unstable in L cells as Cys-βgal produced from Ub-Cys-βgal (Fig. 3*B*; data not shown). Because many ORFs in mammalian DNA encode Met-Cys at the N-termini of apparently cytosolic proteins, it is possible that some of these ORFs encode physiological substrates of the N-end rule pathway.

Initial and Subsequent Decay. The use of UPR confirmed and extended the earlier evidence (6, 18) that the degradation of engineered N-end rule substrates such as X-βgals is nonexponential, the metabolic stability of older X-βgal molecules being higher than the metabolic stability of younger ones (Fig. 3). A likely possibility is that this increase in resistance to proteolysis is caused by the conformational maturation of X-βgal *in vivo*, and also by time-dependent conformational changes of the N-terminal extensions in X-βgals of this and earlier studies (Fig. 1*B*) (2, 6, 18).

The increased accuracy afforded by UPR underscores insufficiency of the current "half-life" terminology, because the *in vivo* degradation of many proteins deviates from first-order kinetics. This is so because a protein molecule *in vivo* is not a fixed structural entity. For example, the probability of degradation of a nascent, partially unfolded, chaperonin-associated protein should be, in

general, different from the probability of degradation of a folded counterpart of this protein at a later time in the same cell. In addition, most proteins undergo covalent modifications and associate with other molecules (including other proteins) in a cell, the fraction of a modified or a complex-associated protein being typically less than unity. Some of these modifications and associations are relevant to the protein's function, whereas the rest are caused by a variety of quasi-random events that include protein damage. Thus, an *in vivo* ensemble of protein molecules encoded by one and the same ORF is inhomogeneous structurally and/or conformationally and, therefore, may not decay exponentially. For some short-lived proteins (e.g., *S. cerevisiae* Matα2p), deviations from first-order decay (at times comparable to a half-life) appear to be small (21). However, many other short-lived proteins, including the engineered N-end rule substrates (Fig. 3), decay with a pronounced nonexponential kinetics (6, 18).

Given the above, we propose a terminology for quantitative aspects of nonexponential decay. For reasons explained below, this terminology is introduced at first in the context of N-end rule substrates such as X-βgals. Specifically, Initial Decay (ID) will denote the ratio of the amount of a labeled X-βgal (normalized against a reference protein) at the end of pulse (time 0) to the (normalized) amount of a labeled long-lived X-βgal, such as Met-βgal, at the same time point (time 0) (Fig. 4). Because ID would, in general, depend on the duration of pulse, an ID-based terminology must invoke the pulse time explicitly. For example, ID^{10} in Table 1 denotes the degradation of an X-βgal relative to Met-βgal at the end of the 10-min pulse. The function of ID is to convey the extent of degradation of a test protein during the pulse (Fig. 4; Table 1).

Subsequent Decay (SD) will denote the ratio of the amount of a labeled test protein at a given chase point to the amount of the same labeled protein at any earlier chase point, including the end of pulse (time 0), with both values corrected against the amounts of a labeled reference protein at the corresponding time points. Thus, for every curve in Fig. 3 (*A–C*), one can calculate SD^{0-60}, SD^{0-120}, and SD^{60-120}, each of these terms addressing different aspects of a nonexponential decay curve for an X-βgal N-end rule substrate.

A single half-life is sufficient for describing first-order decay (22) but is insufficient for describing other decay kinetics, making it necessary to use different ("partial") half-life values for different regions of a decay curve or, alternatively, to employ the complementary ID/SD terminology. In Table 1, the 0- and 60-min data of Fig. 3 *A–C* were used to calculate ID^{10} and SD^{0-60} for 19 different X-βgals. Table 1 also lists the corresponding partial half-lives, calculated for 0–60 min and 0–15 min chase times. The calculation of a partial half-life involves the approximation that the decay of an X-βgal is exponential between the relevant time points. To distinguish between partial half-lives that describe different regions of a decay curve, we propose a generalized half-life term, $t_{0.5}^{y-z}$, where 0.5 denotes the parameter's half-life aspect and *y–z* denotes the relevant time interval (from *y* to *z* min of chase).

In contrast to partial half-lives and SDs, the calculations of which are straightforward for any short-lived protein coexpressed with a reference protein (see the legend to Table 1), the ID term for a short-lived protein can be defined as above only in relation to essentially the same protein that becomes metabolically stable. This would happen, for example, if a normally short-lived protein is expressed in a mutant cell that does not degrade the protein, or if a degron of a short-lived protein is eliminated without altering the number of the protein's methionines and/or other residues that are labeled in a pulse-chase assay. The latter condition holds in the comparisons of short-lived X-βgals with long-lived X-βgals (Fig. 4) but is more difficult to attain for many other short-lived proteins whose degrons remain to be understood. Indeed, the finding that a significant fraction of a short-lived X-βgal is degraded during a pulse resulted from side-by-side comparisons of relative labeling among short-lived and long-lived X-βgals (6, 18).

Applications of UPR. One advantage of the UPR technique is the possibility of comparing the metabolic stabilities of different proteins using pulse data alone (Fig. 4). UPR should also allow the determination of relative metabolic stabilities of proteins *in situ*. In one example of this approach, two nearly identical, separately quantifiable [e.g., fluorescent (23)] reporter proteins that either lack or bear the N-degron would be coproduced in equimolar amounts using UPR. Determining the steady-state molar ratios of these reporters in cell extracts, cells in culture, or individual cells in tissues of transgenic organisms should yield a direct ranking of metabolic stabilities of N-end rule substrates bearing different destabilizing N-terminal residues. Analogous *in situ* UPR assays should be feasible with other short-lived proteins as well.

By increasing the number of Ub moieties in a UPR-based construct, it may be possible to address the long-recognized but poorly understood problem of cotranslational proteolysis. Consider the fusion A-Ub-B-Ub-C, which is analogous to the fusion A-Ub-B in Fig. 1*A* but bears also the second Ub moiety and a C-terminal reporter moiety C. In the absence of cotranslational degradation of this fusion, the molar yield of the N-terminal module A-Ub must be equal to the molar yield of the C-terminal module C. Suppose that a significant fraction of B-Ub-C is degraded processively and cotranslationally (after the cotranslational cleavage by Ub-specific proteases that releases A-Ub). In this case, the molar yield of A-Ub would be higher than that of C, with the difference in yields being a measure of cotranslational proteolysis. A powerful feature of this approach is that it detects a transient kinetic effect such as cotranslational proteolysis by measuring a "static" ratio of two quantities, the yield of A-Ub and the yield of C, in response to alterations of the length, sequence, and degron content of the "spacer" B-Ub. A UPR-based study of cotranslational proteolysis is under way.

We thank L. Larson for her participation at the beginning of this work, M. Ghislain and M. Gonzalez for discussions, and A. Webster for bringing ref. 19 to our attention. We also thank J. Johnston, M. Gonzalez, G. Turner, and A. Webster for their comments on the manuscript. This work was supported by National Institutes of Health Grants DK39520 and GM31530 (to A.V.). F.L. was supported initially by an EMBO postdoctoral fellowship and later by the Swiss National Fund for Research.

1. Hershko, A. & Ciechanover, A. (1992) *Annu. Rev. Biochem.* **61,** 761–807.
2. Varshavsky, A. (1996) *Cold Spring Harbor Symp. Quant. Biol.*, **60,** 461–478.
3. Finley, D., Bartel, B. & Varshavsky, A. (1989) *Nature (London)* **338,** 394–401.
4. Baker, R. T., Tobias, J. W. & Varshavsky, A. (1992) *J. Biol. Chem.* **267,** 23364–23375.
5. Papa, F. R. & Hochstrasser, M. (1993) *Nature (London)* **366,** 313–319.
6. Bachmair, A., Finley, D. & Varshavsky, A. (1986) *Science* **234,** 179–186.
7. Tobias, J. W., Shrader, T. E., Rocap, G. & Varshavsky, A. (1991) *Science* **254,** 1374–1377.
8. Bachmair, A. & Varshavsky, A. (1989) *Cell* **56,** 1019–1032.
9. Gonda, D. K., Bachmair, A., Wünning, I., Tobias, J. W., Lane, W. S. & Varshavsky, A. (1989) *J. Biol. Chem.* **264,** 16700–16712.
10. Jentsch, S. & Schlenker, S. (1995) *Cell* **82,** 881–884.
11. Baker, R. T. & Varshavsky, A. (1995) *J. Biol. Chem.* **270,** 12065–12074.
12. Alagramam, K., Naider, F. & Becker, J. M. (1995) *Mol. Microbiol.* **15,** 225–234.
13. Madura, K. & Varshavsky, A. (1994) *Science* **265,** 1454–1458.
14. de Groot, R. J., Rümenapf, T., Kuhn, R. J., Strauss, E. G. & Strauss, J. H. (1991) *Proc. Natl. Acad. Sci. USA* **88,** 8967–8971.
15. Lemm, J. A., Rümenapf, T., Strauss, E. G., Strauss, J. H. & Rice, C. M. (1994) *EMBO J.* **13,** 2925–2934.
16. Ausubel, F. M., Brent, R., Moore, D. D., Seidman, J. G., Smith, J. A. & Struhl, K. (1992) *Current Protocols in Molecular Biology* (Wiley Interscience, New York).
17. Johnsson, N. & Varshavsky, A. (1994) *EMBO J.* **13,** 2686–2698.
18. Baker, R. T. & Varshavsky, A. (1991) *Proc. Natl. Acad. Sci. USA* **88,** 1090–1094.
19. Ryan, M. D. & Drew, J. (1994) *EMBO J.* **13,** 928–933.
20. Arfin, S. M. & Bradshaw, R. A. (1988) *Biochemistry* **27,** 7979–7984.
21. Hochstrasser, M. & Varshavsky, A. (1990) *Cell* **61,** 697–708.
22. Ross, J. (1995) *Microbiol. Rev.* **59,** 423–450.
23. Heim, R., Cubbit, A. B. & Tsien, R. Y. (1995) *Nature (London)* **373,** 664–665.